Optimal Placement and Capacity of Combined DGs and SCs in Radial Distribution Networks Based on PSO-OS Algorithm

Gonggui Chen, Ao Zhang, Chenxu Zhao, and Zhizhong Zhang *

Abstract— **The distribution of power flow can be effectively improved by optimizing the configuration of Distributed Generators (DGs) and Shunt Capacitors (SCs). Proper placements and capacities of DGs or SCs for real power loss minimization at the radial distribution network (RDN) is attracting more attention as people become more and more dependent on electric power resources. In order to overcome the slow convergence and poor effect of intelligent algorithms in this problem, Particle Swarm Optimization with Orientation and Shrinking factor（PSO-OS） is proposed in this paper. In the suggested PSO-OS algorithm, sensitivity analysis sort of distribution network is introduced to guide the direction of variation to simplify the search space, and shrinking factor is introduced to balance search capabilities in various RDN systems. The proposed method is applied to IEEE-33, IEEE-69 and IEEE-119 systems to solve the problem of simultaneous allocation of DGs and SCs. Simulation results show that the energy loss of the system is reduced and the stability is improved after reconfiguration. By repeating the experiment independently with the traditional PSO algorithm, the comparative analysis of the results proves the superior performance of the improved algorithm. By comparing with the results in recent literature, it reveals the effectiveness of the proposed PSO-OS algorithm in finding the optimal position and capacity of DGs and SCs in the distribution network.**

Index Terms—**Radial distribution network, sensitivity analysis, Distributed Generators (DGs), active and reactive power loss, PSO-OS algorithm.**

I. Introduction

IN recent years, with the large increase of electric energy consumption, the power grid system should not only ensure the safe operation of the power grid, but also meet the needs of users through reasonable design. However, the cost of constructing or upgrading transmission lines and distribution networks is very high, so the installation of distributed generations (DGs) set in the distribution network system is one of the feasible solutions to provide users with greater load capacity [1].

Because the distribution network has the characteristics of low voltage and high current, the energy loss in the power system is relatively large. In this respect, it has been proved that one of the most cost-effective solutions to this problem is to use DG [2]. The research shows that DG can effectively reduce the active power loss during the operation of power grid [3]. The main goal of judging the size and position of DG is to minimize the active and reactive power loss in the distribution network system [4]. On the other hand, voltage quality is also very important for distribution facilities [5, 6].

As a common basic device in power system, shunt capacitors (SCs) have the ability to decrease the network loss of the system, increase the power factor, and improve the node voltage level [7-9]. Consequently, SCs and DGs are often combined to optimize the power grid. If the location or capacity of DGs and SCs are not properly selected, the grid system will be negatively affected [10, 11]. Therefore, the reasonable installation of SCs and DGs unit plays a crucial role in the operation of the power systems.

Various heuristic algorithms have been applied to recent research to optimize power system problems, such as Imperialist Competitive Algorithm (ICA) [12], Hybrid Particle Swarm Optimization (HPSO) [13] and Quasi-oppositional Cuckoo Search Algorithm (QCSA) [14] are used to optimize power flow. Artificial Bee Colony (ABC) [15], Generic Algorithm (GA) [16], and Analytical Method - Particle Swarm Optimization (AM-PSO) [17] are used to study the optimal placements of multiple DGs. In most recent papers, Intelligent Water Drop (IWD) [18], Backtracking Search Optimization Algorithm (BSOA) [19], GA [20] are used for finding the most suitable DGs and SCs placement and capacity parameters and have achieved good results. Moreover, the sensitivity factor is also proposed to help find the optimal solution [21, 22].

In this paper, an improved algorithm PSO-OS is proposed to solve the problem of optimal DGs and SCs configuration. It successfully solves the problems commonly encountered in the previous literature. (1) The iterative convergence of traditional intelligent algorithms in complex power systems takes a long time, and the calculation results are not accurate enough. (2) Although many improved or hybrid algorithms can produce effects on some specific systems, their general applicability is not strong. (3) Directly refer to the sensitivity factor to sort and select the candidate nodes, resulting in the optimization effect cannot reach the best when multiple DGs and SCs are jointly optimized.

Manuscript received June 21, 2020; revised January 22, 2021. This work was supported in part by the Innovation Team Program of Chongqing Education Committee under Grant CXTDX201601019, and in part by the Chongqing University Innovation Team under Grant KJTD201312.

Gonggui Chen is a professor of Key Laboratory of Industrial Internet of Things & Networked Control, Ministry of Education, Chongqing University of Posts and Telecommunications, Chongqing 400065, China; Key Laboratory of Complex Systems and Bionic Control, Chongqing University of Posts and Telecommunications, Chongqing 400065, Chin (e-mail: chenggpower@126.com).

Ao Zhang is a master degree candidate of Chongqing University of Posts and Telecommunications, Chongqing 400065, China (e-mail: zhangaocqupt@163.com).

Chenxu Zhao is a senior engineer of Inner Mongolia Power(Group) Co.,Ltd, Inner Mongolia Power Economy and Technology Research Institute. Hohhot 010010, China; (e-mail: 248349577@qq.com).

Zhizhong Zhang is a professor of Key Laboratory of Communication Network and Testing Technology, Chongqing University of Posts and Telecommunications, Chongqing 400065, China (corresponding author to provide phone: +862362461681; e-mail: zhangzztx@163.com)

In order to solve these problems: (1) The conventional sensitivity factor analysis method is innovatively introduced into the algorithm update mechanism, rather than blindly sorting and then selecting. This not only optimize the search space, reduce the computational complexity but also avoids the problems caused by the collaborative optimization of multiple DGs and SCs. (2) The shrinkage factor is introduced, so that traditional intelligent algorithms can still maintain good general applicability in a variety of computing environments. This makes the PSO-OS algorithm more accurate and efficient for different radial distribution networks.

Meanwhile, three radial distribution networks of IEEE-33, IEEE-69 and IEEE-119 are selected for experimental simulation. The superior performance of the algorithm is verified by comparing and analyzing the calculation results of past literature. On the other hand, the independent repeated experiment comparison between PSO and the improved PSO-OS algorithm proves the success of the algorithm improvement.

II. Problem Formulation

A. Power Flow Formulation

The common RDN with *n* nodes can be represented by the model shown in Fig. 1.

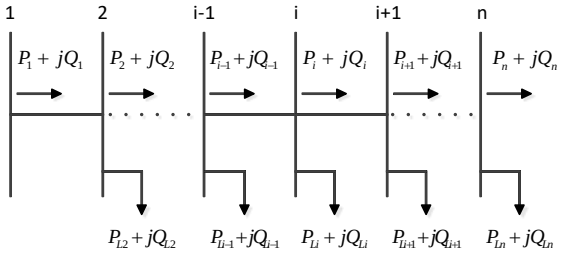

Fig. 1.Abstract diagram of RDN

$$P_{i+1} = P_i - P_{Li+1} - R_{i,i+1} \cdot \frac{P_i^2 + Q_i^2}{|V_i|^2} \tag{1}$$

$$Q_{i+1} = Q_i - Q_{Li+1} - X_{i,i+1} \cdot \frac{P_i^2 + Q_i^2}{|V_i|^2} \tag{2}$$

$$|V_{i+1}|^2 = |V_i|^2 - 2(R_{i,i+1} \cdot P_i + X_{i,i+1} \cdot Q_i) + (R_{i,i+1}{}^2 + X_{i,i+1}{}^2) \cdot \frac{P_i^2 + Q_i^2}{|V_i|^2} \tag{3}$$

where P_i and Q_i are the real and reactive power flowing out of bus i; P_{Li+1} and Q_{Li+1} are the real and reactive load powers at bus i+1. $R_{i,i+1}$ and $X_{i,i+1}$ are the resistance and reactance of the line section between buses i and i+1. $|V_i|$ represents the voltage of bus i.

The power loss in the section of line connecting buses i and i+1 can be computed by the following equations:

$$P_{loss}(i,i+1) = R_{i,i+1} \cdot \frac{P_i^2 + Q_i^2}{|V_i|^2} \tag{4}$$

$$Q_{loss}(i,i+1) = X_{i,i+1} \cdot \frac{P_i^2 + Q_i^2}{|V_i|^2} \tag{5}$$

where P_{loss} is the power loss and Q_{loss} is the reactive power loss. The total power loss of the system, TP_{loss} and TQ_{loss} can be determined by summing up the power losses and the reactive power losses of all line sections of the system, which are given as:

$$TP_{loss} = \sum_{i=1}^{n-1} P_{loss(i,i+1)} \tag{6}$$

$$TQ_{loss} = \sum_{i=1}^{n-1} Q_{loss(i,i+1)} \tag{7}$$

Considering that the research objects are all radial distribution network systems, shown in Fig. 2, the impedance between the preceding node i and the backward node i+1 is expressed as $Z=R_{i,i+1}+jX_{i,i+1}$.

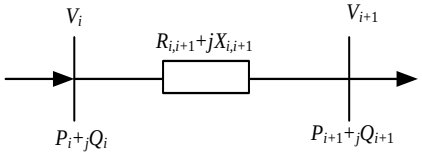

Fig. 2.Abstract diagram between node i and i+1

The influence of active and reactive power on the RDN is represented with the sensitivity factor. And the active and reactive power are injected by the DGs and SCs unit at each node.

The loss sensitivity factors can be calculated by:

$$PLSF = \frac{\partial P_{loss}(i,i+1)}{\partial Q_{i+1}} = \frac{2Q_{i+1}}{|V_{i+1}|^2} R_{i,i+1} \tag{8}$$

$$QLSF = \frac{\partial Q_{loss}(i,i+1)}{\partial Q_{i+1}} = \frac{2Q_{i+1}}{|V_{i+1}|^2} X_{i,i+1} \tag{9}$$

By analyzing the sensitivity of the system and calculating the sensitivity factor of each node, the complexity of optimal selection of the algorithm can be reduced and the optimization time can be saved.

B. Constrains

Power balance: the flow of active and reactive power in all the branches of the system should satisfy Eq. 1 and Eq. 2 respectively. For all branches in the system, the voltage magnitudes at sending and receiving nodes must satisfy Eq. 3.

Any bus voltage must be within the specified maximum and minimum voltage range. Mathematically, it can be expressed as:

$$V_{\min} \le V_i \le V_{\max} \tag{10}$$

where V_{min} and V_{max} are the minimum and maximum voltages allowed by all nodes in the system. The values of these parameters at the systems are set to 0.9 *p.u.* and 1.05 *p.u.* respectively.

$$\frac{\sum_{i=2}^{n} P_i^L - \sum_{i=1}^{N_{DG}} P_i^{DG}}{\sqrt{(\sum_{i=2}^{n} P_i^L - \sum_{i=1}^{N_{DG}} P_i^{DG})^2 + (\sum_{i=2}^{n} Q_i^L - \sum_{i=1}^{N_{SC}} Q_i^{SC})^2}} = \cos\varphi \tag{11}$$

where $cos\varphi$ is the power factor of distribution network. It will be improved when optimal capacity SCs and DGs are placed in the most suitable locations. P_i^L is active load and Q_i^L is reactive load at node i. P_i^{DG} is the capacity of ith DG and Q_i^{SC} is the capacity of ith SC.

$$\sum_{i=1}^{N_{DG}} P_i^{DG} \le 0.8 \times \sum_{i=1}^{n} P_i^L \tag{12}$$

$$\sum_{i=1}^{N_{SC}} Q_i^{SC} \le 0.8 \times \sum_{i=1}^{n} Q_i^L \tag{13}$$

The DGs used in this paper are all generators that can only produce active power (e.g. micro turbines, fuel cells) [23]. The capacity of DGs should not exceed 80 percent of the total active load of the original system, and the reactive power of SCs should never exceed 80 percent of the total reactive load of the original system [24].

III. METHODS

A. Particle Swarm Optimization (PSO)

Proposed in [25], PSO is a global random search algorithm based on swarm intelligence, which is proposed by simulating the migration and clustering behavior of birds in the process of foraging and building its swarm model on the computer to solve the optimization problems.

PSO was inspired from the model of bird foraging and used to solve optimization problems. The potential solution to each optimization problem can be regarded as a bird (particle) in the search space, and each particle has a speed that determines the direction and distance. The particles then follow the current optimal particle and search in the solution space, all of which have a fitness determined by the optimized function.

Step1: For the target search space with dimension D, PSO is the first initialized as a group of random particles (random solutions), including position (X_i) and velocity (V_i).

$$X_i = (x_{i1}, x_{i2}, ..., x_{iD}), \quad i = 1, 2, ..., N \tag{14}$$

$$V_i = (v_{i1}, v_{i2}, ..., v_{iD}), \quad i = 1, 2, ..., N \tag{15}$$

Step2: Calculate the fitness value ($F[i]$) of all particle in the current population. The optimal position searched so far by particle i is called individual extreme value (P_{best}), and the optimal position searched so far by the whole particle swarm is global extreme value (g_{best}).

$$P_{best} = (p_{i1}, p_{i2}, ..., p_{iD}), \quad i = 1, 2, ..., N \tag{16}$$

$$g_{best} = (g_{i1}, g_{i2}, ..., g_{iD}), \quad i = 1, 2, ..., N \tag{17}$$

Step3: Update the velocity and position according to the particle update formula. Where c_1 and c_2 are learning factors, also known as acceleration constant, ω is inertia factor, r_1 and r_2 are uniform random numbers within the range of [0,1].

$$V_{id}^{k+1} = \omega V_{id}^{k} + c_1 r_1 (P_{id}^{k} - X_{id}^{k}) + c_2 r_2 (P_{gd}^{k} - X_{id}^{k}) \tag{18}$$

$$X_{id}^{k+1} = X_{id}^{k} + V_{id}^{k+1} \tag{19}$$

Step4: Determine whether the end condition is satisfied (generally the convergence of the target function or the upper limit of the number of iterations), otherwise return to the Step2.

B. Particle Swarm Optimization with Orientation and Shrinking factor（PSO-OS）

In the original PSO algorithm, multiple location and capacity parameters of the DGs and SCs will be incorporated into the research process, which will increase the dimension and complexity. Moreover, since the alternate locations of DGs/SCs are discrete values, it is even more difficult for the algorithm to determine the optimal locations and optimal capacities at the same time.

(1). Orientation variation based on sensitivity analysis results

In the conventional PSO algorithm, we often add a random variation to improve the global search ability of the algorithm, which can avoid falling into the local optimal situation due to the random initialization of the population. However, this kind of undifferentiated variation without orientation cannot meet the needs of the problem. In this paper, a new guidance variation method based on network loss sensitivity analysis results is proposed, which can be used to select the optimal combination of DGs/SCs placement node locations.

Through Eq. 8 and Eq. 9, the loss sensitivity factors can be calculated. They can indicate the effect of the nodes to decrease the power loss of the radial distribution system when injecting active/reactive power by DGs/SCs. But it doesn't mean that picking the first and second most sensitive nodes is the best combination.

Although the selection of node locations cannot be simply based on the order of sensitivity, the best combination of locations is made up of nodes with high sensitivity. Therefore, the nodes are sorted from high to low in terms of active power/reactive power network loss sensitivity and divided into 3 classes on average: class-1, class-2 and class-3. Every time the variations of locations are identified, the probability of choosing one of the three classes is 60% for class-1, 30% for class-2 and 10% for class-3.

This new strategy not only considers the ranking of the sensitivity factors of each bus, which improves the search efficiency of the algorithm, but also considers the nodes with lower priority to ensure that no feasible solutions are missed.

(2). Shrinking factor

$$V_{id}^{k+1} = \omega V_{id}^{k} + \xi (c_1 r_1 (P_{id}^{k} - X_{id}^{k}) + c_2 r_2 (P_{gd}^{k} - X_{id}^{k})) \tag{20}$$

$$\xi = \frac{2}{\left| 2 - c - \sqrt{c^2 - 4c} \right|}, \quad c = c_1 + c_2 \tag{21}$$

The learning factors c_1 and c_2 determine the influence of the experience information of the particle itself and other particles on the particle trajectory, reflecting the information communication between the particle swarm. If a larger value of c_1 is set, the particle will linger in the local scope for a long time, while a larger value of c_2 will cause the particle to converge to the local minimum value prematurely. By introducing the compression factor and selecting appropriate parameters, the flying speed of particles can be controlled effectively, so the algorithm can achieve an effective balance between global detection and local mining. Update the formula as Eq. 20 and Eq. 21, and ξ is the shrinking factor.

```
Input: objective function: F[i],
       Initial population: pop = [C_DG1, ..., L_SCj]
       initialize the parameters of PSO-OS: c1,c2,max
       Sensitivity ranking matrix: R = [node_fist , ... ,node_last ]
Begin
   Part1: Generate candidate node or combination
      for Cycle =1:max
         while (k < iter_number)
            Update F[i], P_best, g_best
            Guaranteed to meet constraints
         end while
            Records of the results
      end for
   Part2: Generate capacity for each candidate node
      Select the candidate results from part1
      while (k < iter_number)
            Update F[i], P_best, g_best
            Guaranteed to meet constraints
      end while
End
```

Fig. 3.Pseudo code of the proposed method

C. Method realization flow

The pseudo-code of optimization algorithm and flow chart are shown in Fig. 3 and Fig. 4 respectively. The whole algorithm process will be divided into two parts. The first part will generate three alternative node combinations, and the second part will conduct optimal DGs/SCs capacity configuration for these candidate node combinations. Finally, the combination with minimum active power network loss will be selected as the output result.

Specifically, the sensitivity analysis of active/reactive power loss is performed for a given radial distribution network system. In the first optimization, the population is initialized as Eq. 22 randomly, and fitness value is given as Eq. 23.

$$pop = [C_{DG1} \dots C_{DGi}\ , C_{SC1} \dots C_{SCj}\ , L_{DG1} \dots L_{DGi}\ , L_{SC1} \dots L_{SCj}] \tag{22}$$

$$F_{[i]} = \sum_{i=1}^{n-1} R_{i,i+1} \cdot \frac{P_i^2 + Q_i^2}{|V_i|^2} \tag{23}$$

where C_{DGi} is the capacity of ith DG and C_{SCj} is the capacity of jth SC. L_{DGi} is the location of ith DG and L_{SCj} is the location of jth SC. Then, individual extreme value (P_{best}) and global extreme value (g_{best}) are recorded for minimum real power loss. If the number of iterations is not reached after the results are treated out of bounds, the location data will be subject to instructive variation, and the capacity data will be subject to random variation to enter the next round of update iteration. Through the loop control of variable cycle, multiple groups of maximum connection capacity and position combination will be generated, and the three combined positions with the minimum network loss will be taken as the position data of the next round of optimization. In the second round of optimization, since the position of DGs/SCs has been fixed, only the optimal capacity needs to be obtained, so it is easier to get accurate results. Finally, the minimum real power loss in the three independent optimization results is selected as the final output.

The advantages of this method are as follows:

(1) It avoids the difficulty of exponential growth of search space due to the large dimension. (2) Separate locations and capacities to reduce the difficulty of calculation and improve the accuracy of results. (3) The analysis result of network loss sensitivity is introduced as a guide, which makes the search direction develop towards the region with higher possibility and improves the search efficiency.

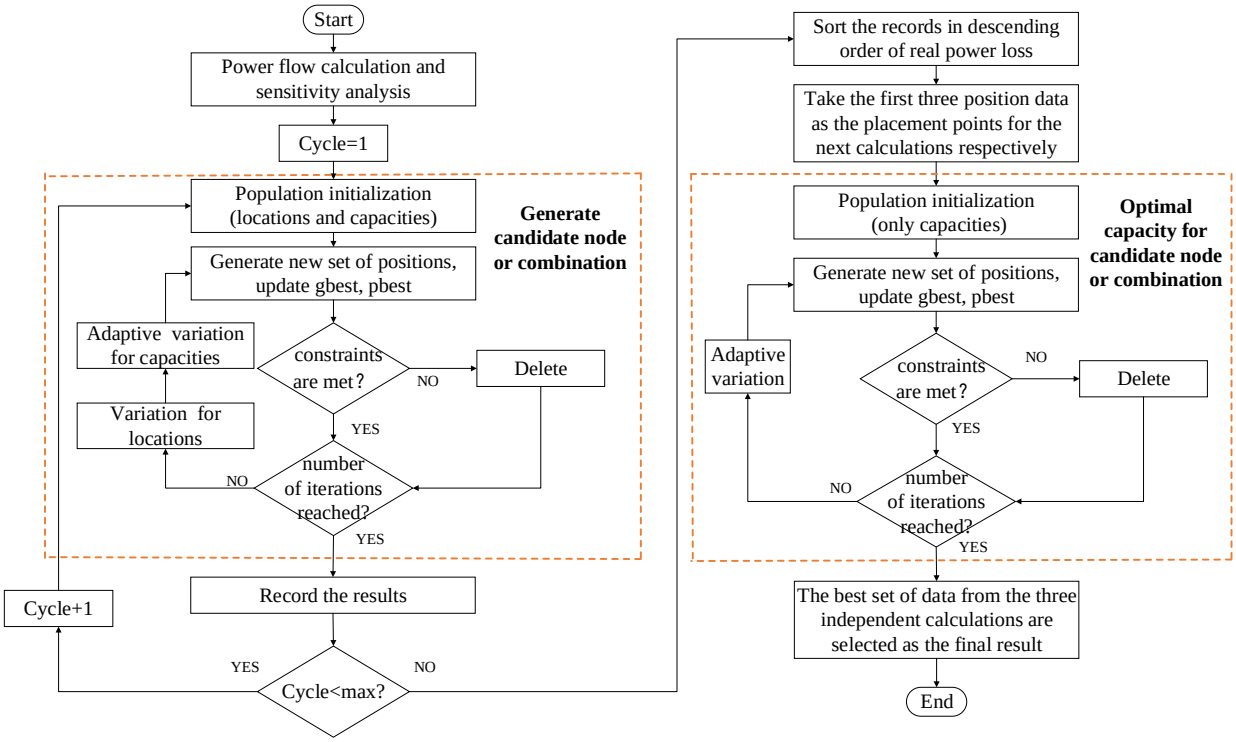

Fig. 4. Flow chart for PSO-OS

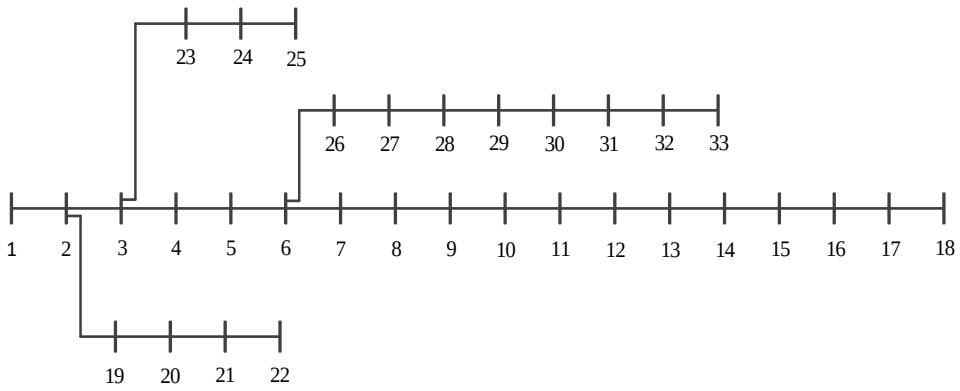

Fig. 5. IEEE-33 bus test system

IV. Simulation Results and Discussion

The method proposed in this paper is verified by three systems, which are IEEE-33 bus, IEEE-69 bus and IEEE-119 bus system respectively. And the total range of DGs/SCs for each system and the individual range of DGs/SCs are given in TABLE I, IV, and VII.

A. IEEE-33 bus radial distribution network

The line data and load data in the test system are obtained from [26]. The system is a balanced three-phase radial network composed of 33 nodes and 32 branches. The reference voltage of the system is 12.66KV, the total active load of the system is 3.7MW, and the reactive load is 2.3MVAR. The single line diagram of the IEEE-33 bus test system is shown in Fig. 5. The detailed information of DGs/SCs on IEEE-33 nodes under various research conditions is provided in TABLE I.

TABLE I
Introduction Of Various Cases For Ieee-33 System

	case no.	number of DGs	number of SCs	size range of DGs	size range of SCs
IEEE -33	case-1	0	1	--	0-1.84MVAR
	case-2	0	3	--	0-1.84MVAR
	case-3	1	0	0-2.96MW	--
	case-4	2	0	0-2.96MW	--
	case-5	3	0	0-2.96MW	--
	case-6	1	1	0-2.96MW	0-1.84MVAR
	case-7	2	2	0-2.96MW	0-1.84MVAR
	case-8	3	3	0-2.96MW	0-1.84MVAR

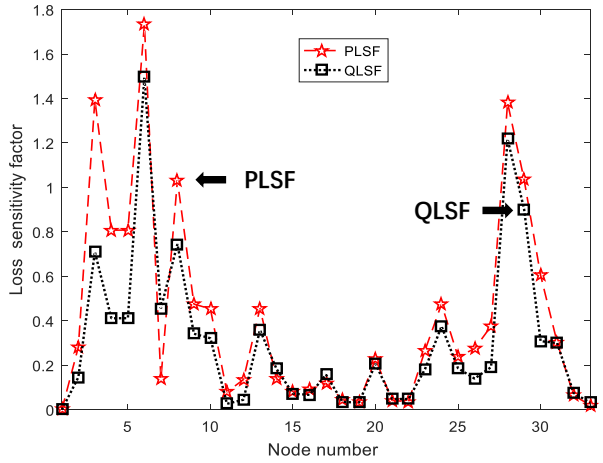

Fig. 6.Distribution of sensitivity factors in IEEE-33

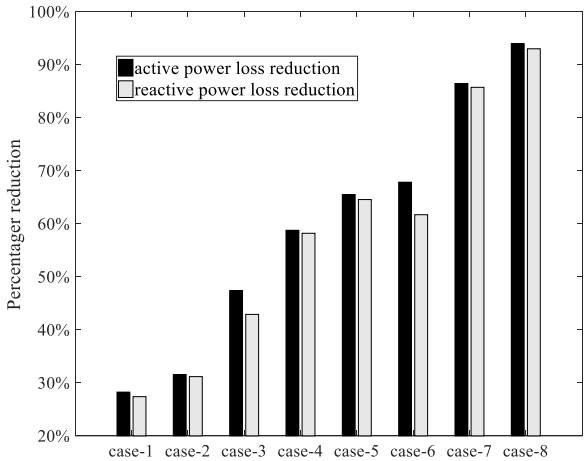

Fig. 7. Active/reactive network loss reduction of each case in IEEE-33 systems

By calculating the loss sensitivity factor of IEEE-33 node test system, the result is shown in Fig. 6. As the original node, the number of nodes in the remaining 32 nodes is roughly the same as that of the active/reactive network loss sensitivity factors of each node. Node 6 has the highest sensitivity of active/reactive power loss and it is considered as the best candidate node in case-3 and case-6. Other selected nodes, such as 13, 24 and 30, are also the nodes with relatively high sensitivity.

In order to verify the effectiveness of the hybrid method, a variety of tests are carried out for the small-scale distribution network with 33 nodes. In the original IEEE-33 system, the real power loss and reactive power loss are 211KW and 143.1KVAR respectively, and the lowest node of the system voltage is 0.9037 *p.u.* (at node 18).

TABLE II shows the data of multiple test results. It can be clearly seen from the results that only SCs configuration of the system can improve the grid node voltage and reduce the active/reactive power loss, but the amplitude is limited and the real power loss reduction can only reach 31.56% for 3 SCs. As the number of DG increases, the active power loss of the system decreases significantly, and the worst voltage can be further improved when the system is configured only for DGs. In case-5, both active and reactive power loss of the system decrease by 65.5% and 64.57%, and the lowest voltage is 0.9687 *p.u.* at bus 33.

Furthermore, the optimization effect is further improved when both the DG and SC are considered as optimization units. It is easy to see from case-6 that when only one DG and one SC are added to the system, the effect is similar to that of adding DGs with different capacity in three nodes at the same time. In case-8, the 13, 25 and 30 nodes are all placed in DGs and SCs. At this time, the active/reactive power loss of the system is reduced to 6.02% and 6.99% of the original system, and the voltage distribution is greatly improved. The minimum voltage deviation of case-8 is also well improved to 0.9924 *p.u.* at bus 8.

It can be observed from Fig. 7 that the active/reactive power injected into the system changes the power flow distribution and reduces the active and reactive power loss of the original power system. Among them, the optimization effect is the best when the DGs and SCs are put into the system at the same time. In addition, because of the high installation cost of a single DG, it is not feasible to place large number of DGs in the actual distribution network optimization. Therefore, DGs and SCs are usually configured in the system at the same time to improve the network performance.

The voltage distribution of all nodes under partial test conditions is shown in Fig. 8. It can be observed that, in addition to the significant improvement in the voltage of the node where the DGs/SCs are placed, the voltage amplitude of other nodes is also increased differently (and all voltages are within the constraint range). What's more, since the active load of the original system is 3.7WM and the reactive load is 2.3MVAR, adding DGs can better improve the performance index of the grid system than adding SCs. However, considering the installation, maintenance and related supporting costs of DG, the best solution should be to jointly optimize the distribution network system for DGs and SCs.

TABLE III compares the proposed algorithm with other algorithms, PSO-OS has better performance for real/reactive power loss and improving the minimum voltage of the test system than other algorithms. For example, when the total

size of the capacitors is similar, in the same test system where only the SCs are configured, the active network loss of the system is 7.3KW which is less than that of the BPSO method Furthermore, when only the DGs are configured, PSO-OS and HYBRID select the same installation nodes 30,24 and 14, but PSO-OS selects better in specific capacity configuration, with lower active network loss (72.79 KW vs. 72.81 KW) and higher minimum voltage (0.9687 *p.u.* vs. 0.9684 *p.u.*). Similarly, the method proposed in this paper is still superior in terms of active power network loss and minimum voltage when faced with different DGs configuration schemes of installation node given by BFOA. For case-7, when the DGs and SCs are selected simultaneously (two DGs of 1085KW at node 30 and 846KW at node 13, two SCs of 1073KVAR at node 30 and 388KVAR at node 13), the system active network loss is reduced to 28.6 KW with a minimum voltage of 0.9801 *p.u.* at node 25. Compared with the scheme proposed by IMED, both the network loss (32.08 KW) and the minimum voltage (0.979 *p.u.*) show that the proposed PSO-OS algorithm gives much better performance. In the same way, in the face of three DGs and three SCs, the method proposed in this article is still able to give a better solution than IPSO and BFOA, which reflects the superiority of PSO-OS.

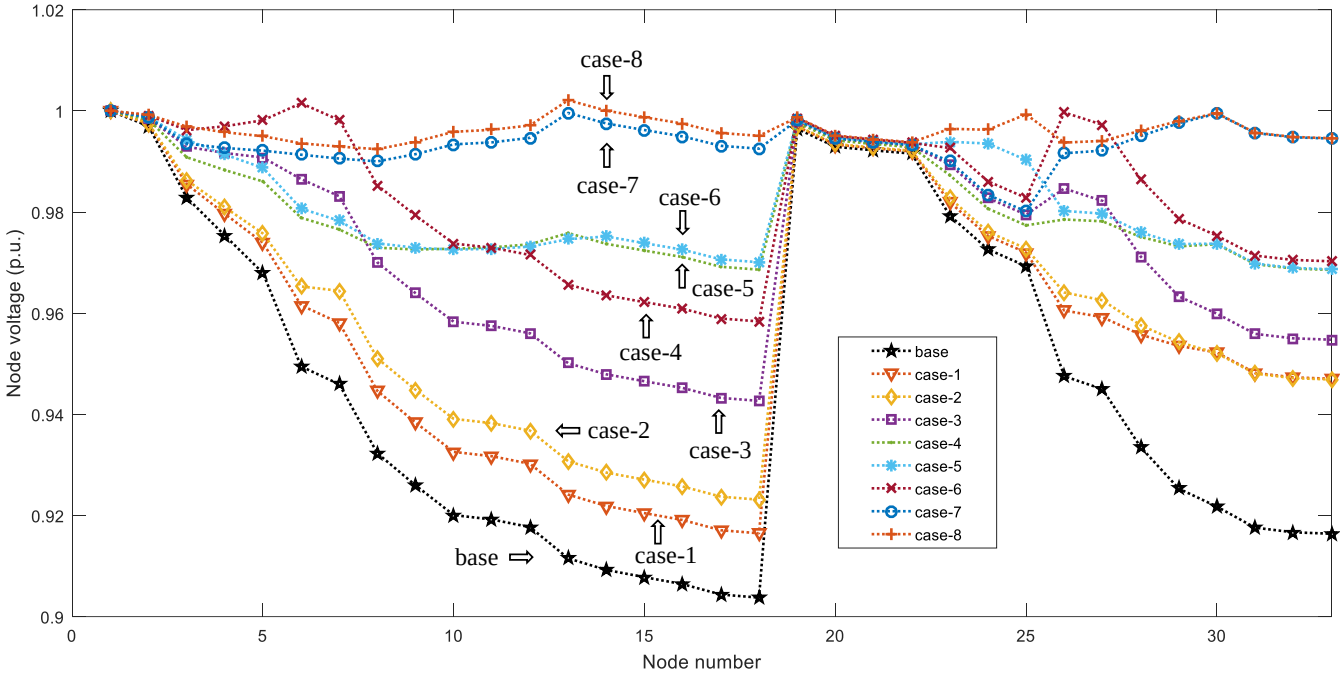

Fig. 8. Voltage distribution in IEEE-33

TABLE II
COMPARISON OF PSO-OS AND OTHER LITERATURE ALGORITHMS FOR IEEE-33 SYSTEM

case		PSO-OS	BPSO[27]	IPSO[28]	IMDE[29]	HYBRID[30]	BFOA[31]
SC only	real power loss (KW)	**144.4**	151.7				
	size of SC in KVAR (node)	651(7), 291(29) 720(30)	610(14) 920(33)				
	min voltage in p.u.(node)	0.9231(18)	0.935(18)				
case-3 (single DG)	real power loss (KW)	**111**				111.03	
	size of DG in KW (node)	2579(6)				2598(6)	
	min voltage in p.u.(node)	0.9427(18)				0.9425(18)	
case-4,5 (multiple DG)	real power loss (KW)	**72.79**	111.5		84.28	72.81	98.3
	size of DG in KW (node)	1066(30) 1098(24),772(14)	520(8) 1300(33)		840(14) 1130(30)	1068(30), 1073(24),755(14)	633(7),90(18) 947(33)
	min voltage in p.u.(node)	0.9687(33)	0.919(18)		0.971(33)	0.9684(33)	0.9645
case-7 (2DG +2SC)	real power loss (KW)	**28.6**			32.08		
	size of DG in KW (node)	1085(30) 846(13)			1080(10) 896.4(31)		
	size of SC in KVAR (node)	1073(30) 388(13)			254.8(16) 932.3(30)		
	min voltage in p.u.(node)	0.9801(25)			0.979(25)		
case-8 (3DG +3SC)	real power loss (KW)	**12.7**		13.4			41.41
	size of DG in KW (node)	1002(30) 828(13),804(25)		831(14),1005(24) 1128(30)			542(17),160(18) 895(33)
	size of SC in KVAR (node)	1020(30),404(13) 405(25)		300(14),600(24) 1200(30)			163(18),541(30) 338(33)
	min voltage in p.u.(node)	0.9924(8)		0.9783			0.9783

TABLE III
SIMULATION RESULTS OF VARIOUS CASES FOR IEEE-33 SYSTEM

Control variables	**base**	**case-1**	**case-2**	**case-3**	**case-4**	**case-5**	**case-6**	**case-7**	**case-8**
DG1(KW)	--	--	--	2579 (6)	1159 (30)	1066 (30)	2560(6)	1085 (30)	1002 (30)
DG2(KW)	--	--	--	--	852 (13)	1098 (24)	--	846 (13)	828 (13)
DG3(KW)	--	--	--	--	--	772 (14)	--	--	804 (25)
SC1(KVAR)	--	1258 (30)	651 (7)	--	--	--	1762(6)	1073 (30)	1020 (30)
SC2(KVAR)	--	--	291 (29)	--	--	--	--	388 (13)	404 (13)
SC3(KVAR)	--	--	720 (30)	--	--	--	--	--	405 (25)
V1(p.u.)	1	1	1	1	1	1	1	1	1
V2(p.u.)	0.997014	0.997435	0.997561	0.998593	0.998268	0.998811	0.999120	0.998702	0.999233
V3(p.u.)	0.982882	0.985521	0.986315	0.992915	0.990843	0.994299	0.996196	0.993547	0.996908
V4(p.u.)	0.975372	0.979652	0.980945	0.991670	0.988302	0.991373	0.996965	0.992668	0.995779
V5(p.u.)	0.967946	0.973935	0.975751	0.990777	0.986052	0.988722	0.998150	0.992138	0.994988
V6(p.u.)	0.949468	0.961562	0.965284	0.986513	0.978879	0.980683	1.001510	0.991338	0.993591
V7(p.u.)	0.945943	0.958085	0.964435	0.983130	0.976562	0.978279	0.998182	0.990574	0.992936
V8(p.u.)	0.932287	0.944614	0.951058	0.970024	0.972951	0.973814	0.985286	0.990017	0.992444
V9(p.u.)	0.925954	0.938368	0.944856	0.963949	0.972592	0.972938	0.979309	0.991447	0.993908
V10(p.u.)	0.920080	0.932574	0.939103	0.958314	0.972754	0.972573	0.973765	0.993380	0.995871
V11(p.u.)	0.919211	0.931717	0.938253	0.957480	0.973009	0.972729	0.972945	0.993781	0.996263
V12(p.u.)	0.917696	0.930223	0.936769	0.956027	0.973628	0.973158	0.971516	0.994676	0.997138
V13(p.u.)	0.911521	0.924132	0.930722	0.950105	0.975849	0.974633	0.965690	0.999599	1.002122
V14(p.u.)	0.909230	0.921874	0.928480	0.947909	0.973712	0.975172	0.963530	0.997513	1.000041
V15(p.u.)	0.907804	0.920467	0.927083	0.946541	0.972380	0.973842	0.962184	0.996213	0.998745
V16(p.u.)	0.906422	0.919104	0.925730	0.945216	0.971091	0.972555	0.960881	0.994955	0.997490
V17(p.u.)	0.904373	0.917084	0.923725	0.943252	0.969180	0.970647	0.958949	0.993090	0.995630
V18(p.u.)	0.903760	0.916479	0.923124	0.942664	0.968607	0.970075	0.958371	0.992531	0.995073
V19(p.u.)	0.996486	0.996907	0.997033	0.998066	0.997740	0.998284	0.998593	0.998174	0.998706
V20(p.u.)	0.992908	0.993331	0.993457	0.994494	0.994167	0.994712	0.995023	0.994603	0.995136
V21(p.u.)	0.992204	0.992626	0.992753	0.993790	0.993463	0.994009	0.994320	0.993899	0.994433
V22(p.u.)	0.991566	0.991989	0.992116	0.993154	0.992827	0.993373	0.993684	0.993263	0.993797
V23(p.u.)	0.979296	0.981945	0.982742	0.989367	0.987286	0.993892	0.992659	0.990004	0.996460
V24(p.u.)	0.972625	0.975291	0.976094	0.982764	0.980670	0.993549	0.986079	0.983402	0.996270
V25(p.u.)	0.969299	0.971975	0.972780	0.979473	0.977372	0.990294	0.982803	0.980114	0.999316
V26(p.u.)	0.947538	0.960528	0.964093	0.984660	0.978528	0.980215	0.999687	0.991622	0.993736
V27(p.u.)	0.944974	0.959216	0.962560	0.982198	0.978172	0.979694	0.997264	0.992148	0.994068
V28(p.u.)	0.933532	0.955749	0.957625	0.971212	0.975081	0.975988	0.986452	0.995017	0.996079
V29(p.u.)	0.925312	0.953541	0.954298	0.963320	0.973228	0.973662	0.978686	0.997576	0.997991
V30(p.u.)	0.921754	0.952226	0.952075	0.959904	0.973625	0.973757	0.975324	0.999466	0.999532
V31(p.u.)	0.917592	0.948198	0.948047	0.955909	0.969686	0.969819	0.971393	0.995631	0.995697
V32(p.u.)	0.916676	0.947312	0.947160	0.955030	0.968820	0.968953	0.970528	0.994787	0.994854
V33(p.u.)	0.916392	0.947038	0.946886	0.954758	0.968552	0.968684	0.970260	0.994526	0.994592
min voltage (node)(p.u.)	0.9037(18)	0.9165(18)	0.9231(18)	0.9427(18)	0.9686(18)	0.9687(33)	0.9583(18)	0.9801(25)	0.9924(8)
max voltage (node)(p.u.)	1(1)	1(1)	1(1)	1(1)	1(1)	1(1)	1.0015(6)	1(1)	1.0021(13)
Real power loss (KW)	**211**	**151.4**	**144.4**	**111**	**87**	**72.79**	**67.86**	**28.6**	**12.7**
Reactive power loss (KVAR)	143.1	103.9	98.5	81.7	59.8	50.7	54.8	20.4	10

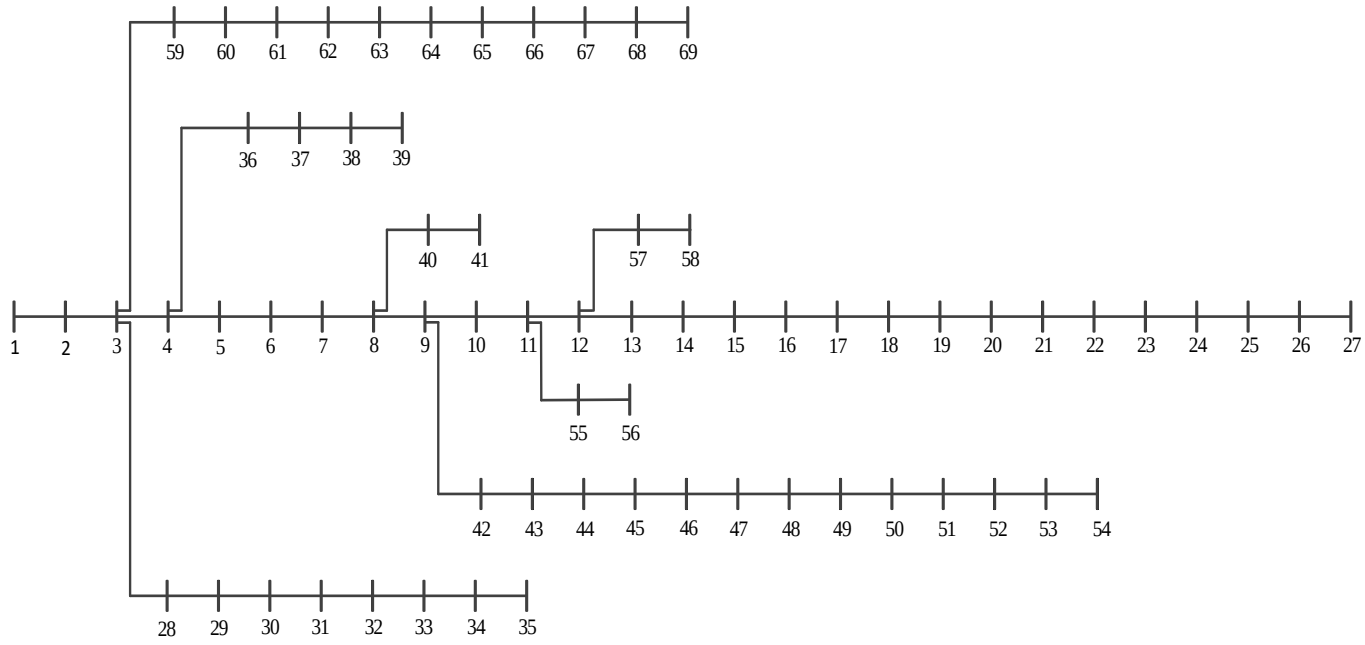

Fig. 9.IEEE-69 bus test system

B. IEEE-69 bus radial distribution network

The line data and load data in the test system are obtained from [32]. The system is a balanced three-phase radial network composed of 69 nodes and 68 branches. The reference voltage of the system is 12.66KV, the total active load of the system is 3.8MW, and the reactive load is 2.7MW. The single line diagram of the IEEE-69 bus test system is shown in Fig. 9. The detailed information of DGs/SCs on IEEE-69 nodes under various research conditions is provided in TABLE IV.

TABLE IV
INTRODUCTION OF VARIOUS CASES FOR IEEE-69 SYSTEM

	case no.	number of DG	number of SC	size range of DGs	size range of SCs
IEEE -69	case-9	0	1	--	0-2.16MVAR
	case-10	0	3	--	0-2.16MVAR
	case-11	1	0	0-3.04MW	--
	case-12	2	0	0-3.04MW	--
	case-13	3	0	0-3.04MW	--
	case-14	1	1	0-3.04MW	0-2.16MVAR
	case-15	2	2	0-3.04MW	0-2.16MVAR
	case-16	3	3	0-3.04MW	0-2.16MVAR

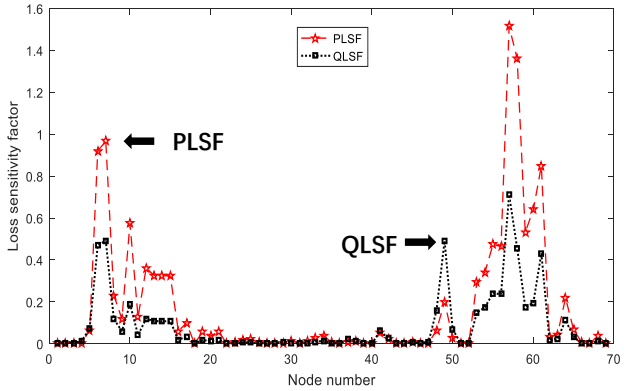

Fig. 10. Distribution of sensitivity factors in IEEE-69

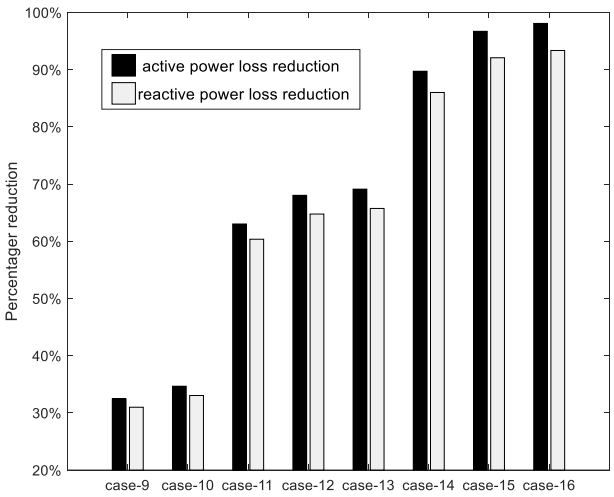

Fig. 11. Active/reactive network loss reduction of each case in IEEE-69 systems

By calculating the active and reactive sensitivity factor of the IEEE-69 test system, the result is shown in Fig. 10. The proposed algorithm avoids taking sensitivity factor ranking as the only criterion to determine the final optimization result, which makes the improved PSO-OS algorithm have better global search capabilities. It can be observed that most of the selected nodes belong to nodes with high sensitivity, such as node 61, 60 and 15, but there are also nodes with low sensitivity, such as node 18. This indicates that the sensitivity analysis-oriented variation method is correct and can still be considered comprehensively in the selection process.

In order to prove that this method is also applicable to other distribution network systems, this paper adopts the same 8 cases for simulation experiments for IEEE-69 system. In the original IEEE-69 system, the real power loss and reactive power loss are 224.95KW and 102.14KVAR respectively, and the lowest voltage is 0.9092 *p.u.* at node 65.

Fig. 11 shows the percentage of active/reactive network loss reduction in each case. It can be seen, placing the single DG (case-11) with the best capacity at the same node (the best location) has a better effect than placing the best capacity SC (case-9). For cases with SCs only, the distribution of SCs in case-10 is more complicated than in case-9, and the total capacitance is 34% more than in case-9, but there is little improvement in the worst voltage (from 0.9307 *p.u.* to 0.9315 *p.u.*) and only 2.22% reduction in active/reactive network loss. This is not economical or feasible in practical optimization measures. In the case that the amount of DG is the same and the total installed capacity is similar, the introduction of reactive power with lower unit cost plays a crucial role in the reduction of network loss and contributes to the improvement of voltage.

TABLE V shows the data of multiple cases results. It should be specially pointed out that in order to control the length of the table, the branch voltage is replaced by the average voltage of all nodes in the branch. For example, $V_{13\text{-}27}$ represents the average voltage from node 13 to node 27.

From case-9 to case-13, it shows that simply increase the capacity/number of SCs or DGs cannot further improve the optimization effect of the system very well. For example, in case-13, three locations are selected to place generators of different capacities (634KW at node 11, 348KW at node 21, 1744KW at node 61), resulting in a 69.1% reduction in the active network loss of the system. However, in the case-14, only placing one DG and one SC with capacities of 1834KW and 1308KVAR at node 61 could reduce the active power loss by 89.71%. As a result, the best solution is to combine the SCs with the DGs, which is more practical.

Fig. 12 shows the voltage distribution of each node. Although a few nodes have slight overshoot under case-14, case-15 and case-16, the voltage of most nodes has been greatly improved and the overshoot is within the acceptable range.

The successful optimization is shown in TABLE VI. The PSO-OS algorithm proposed in this paper also has better performance in IEEE-69 system. In case-14, when node 61 is also selected by MOEA/D as the placement node for SC and DG, the PSO-OS algorithm had a smaller network loss (23.14KW vs. 23.17KW). Moreover, in case-15, two DGs (1700KW at node 61 and 547KW at node 17) and two SCs (1256KVAR at node 61 and 421KVAR at node 17) are installed with worst node voltage of 0.9943 *p.u.* and real power loss of 7.45KW. In IMED, two DGs and two SCs are also installed, but the minimum voltage is 0.9915 *p.u.* and the net loss is 13.83KW. Similarly, the PSO-OS algorithm proposed in this paper can also provide a better configuration with lower network loss scheme when facing the optimization problem of three DGs and three SCs.

These results clearly certificate that the PSO-OS method can give a better performance than other algorithms.

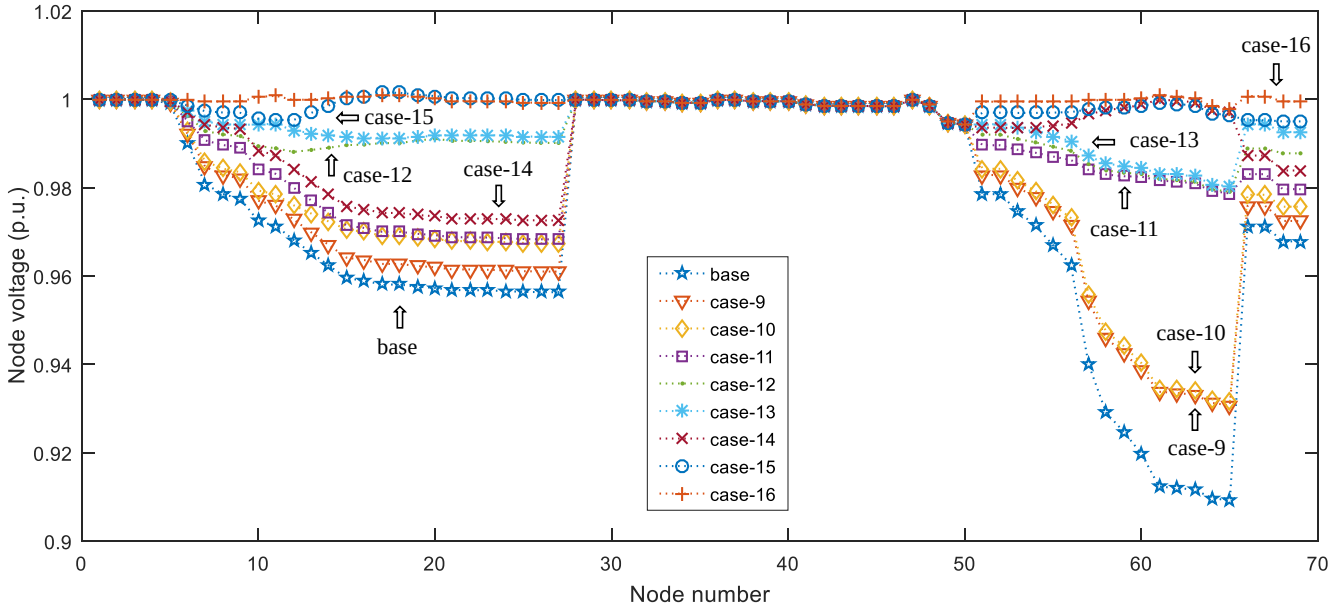

Fig. 12. Voltage distribution in IEEE-69

TABLE V
SIMULATION RESULTS OF VARIOUS CASES FOR IEEE-69 SYSTEM

Control variables	**base**	**case-9**	**case-10**	**case-11**	**case-12**	**case-13**	**case-14**	**case-15**	**case-16**
DG1(KW)	--	--	--	1867(61)	1790(61)	634(11)	1834(61)	1700(61)	553(11)
DG2(KW)	--	--	--	--	505(20)	348(21)	--	547(17)	383(18)
DG3(KW)	--	--	--	--	--	1744(61)	--	--	1686(61)
SC1(KVAR)	--	1330(61)	471(15)	--	--	--	1308(61)	1256(61)	422(11)
SC2(KVAR)	--	--	433(60)	--	--	--	--	421(17)	245(18)
SC3(KVAR)	--	--	880(61)	--	--	--	--	--	1197(61)
V1(p.u.)	1	1	1	1	1	1	1	1	1
V2(p.u.)	0.999967	0.999977	0.999981	0.999973	0.999975	0.999976	0.999983	0.999987	0.999990
V3(p.u.)	0.999933	0.999954	0.999961	0.999947	0.999949	0.999952	0.999967	0.999975	0.999980
V4(p.u.)	0.999840	0.999892	0.999909	0.999873	0.999880	0.999887	0.999924	0.999944	0.999957
V5(p.u.)	0.999021	0.999334	0.999439	0.999380	0.999457	0.999532	0.999679	0.999836	0.999939
V6(p.u.)	0.990086	0.992152	0.992821	0.995110	0.996198	0.997266	0.997017	0.998589	0.999729
V7(p.u.)	0.980794	0.984687	0.985949	0.990686	0.992829	0.994936	0.994254	0.997299	0.999519
V8(p.u.)	0.978578	0.982914	0.984320	0.989649	0.992048	0.994407	0.993617	0.997019	0.999501
V9(p.u.)	0.977445	0.982017	0.983500	0.989146	0.991682	0.994176	0.993327	0.996920	0.999540
V10(p.u.)	0.972447	0.977043	0.979356	0.984209	0.989401	0.994360	0.988412	0.995593	1.000528
V11(p.u.)	0.971346	0.975947	0.978450	0.983121	0.988921	0.994443	0.987329	0.995330	1.000794
V12(p.u.)	0.968187	0.972803	0.976023	0.980001	0.988104	0.992933	0.984222	0.995329	0.999816
$V_{13\text{-}27}$(p.u.)	0.958222	0.962887	0.969071	0.970159	0.990101	0.991669	0.974423	1.000124	0.999986
$V_{28\text{-}35}$(p.u.)	0.999602	0.999621	0.999628	0.999613	0.999616	0.999619	0.999633	0.999642	0.999647
$V_{36\text{-}39}$(p.u.)	0.999704	0.999721	0.999728	0.999713	0.999716	0.999719	0.999733	0.999742	0.999747
$V_{40\text{-}41}$(p.u.)	0.999192	0.999213	0.999220	0.999206	0.999208	0.999211	0.999225	0.999234	0.999239
$V_{42\text{-}54}$(p.u.)	0.990978	0.992574	0.993528	0.995035	0.995078	0.996516	0.996497	0.997538	0.998317
$V_{55\text{-}56}$(p.u.)	0.964758	0.973157	0.974653	0.986659	0.988816	0.991088	0.994262	0.997052	0.999453
$V_{57\text{-}58}$(p.u.)	0.934570	0.950150	0.951679	0.983498	0.984636	0.986303	0.997079	0.997858	0.999803
$V_{59\text{-}69}$(p.u.)	0.934346	0.949145	0.950833	0.981135	0.983958	0.986648	0.993892	0.997018	0.999866
min voltage	0.9092(65)	0.9307(65)	0.9315(65)	0.9683(27)	0.9791(65)	0.9803(65)	0.9726(27)	0.9943(50)	0.9943(50)
max voltage	1(1)	1(1)	1(1)	1(1)	1(1)	1(1)	1(1)	1.00149(17)	1.00086(18)
Real power loss (KW)	**224.95**	**152**	**147**	**83.2**	**71.94**	**69.5**	**23.14**	**7.45**	**4.34**
Reactive power loss (KVAR)	102.14	70.5	68.4	40.5	36	35	14.3	8.1	6.8

TABLE VI
COMPARISON OF PSO-OS AND OTHER LITERATURE ALGORITHMS FOR IEEE-69 SYSTEM

case		PSO-OS	MOEA/D[21]	IMDE[29]	IPSO[28]
case-14 (1DG+ 1SC)	real power loss in KW	**23.14**	23.17		
	size of DG in KW (node)	1834(61)	1829(61)		
	size of SC in KVAR (node)	1308(61)	1301(61)		
	min voltage in p.u.(node)	0.9726(27)	0.9731(27)		
case-15 (2DG+ 2SC)	real power loss in KW	**7.45**		13.83	
	size of DG in KW (node)	1700(61), 547(17)		1738(62), 479(24)	
	size of SC in KVAR (node)	1256(61), 421(17)		1192(61), 109(63)	
	min voltage in p.u.(node)	0.9943(50)		0.9915(68)	
case-16 (3DG+ 3SC)	real power loss in KW	**4.34**			4.37
	size of DG in KW (node)	553(11), 383(18), 1686(61)			557(11), 321(21), 1672(61)
	size of SC in KVAR (node)	422(11), 245(18), 1197(61)			300(11), 300(18), 1200(61)
	min voltage in p.u.(node)	0.9943(50)			0.9943(50)

C. IEEE-119 bus radial distribution network

The system is a balanced three-phase radial network composed of 119 nodes and 118 branches. The reference voltage of the system is 12.66KV, the total active load of the system is 23.68MW, and the reactive load is 17.76MW. The single line diagram of the IEEE-119 bus test system is shown in Fig. 13.

TABLE VII
INTRODUCTION OF VARIOUS CASES FOR IEEE-119 SYSTEM

	case no.	number of DG	number of SC	size range of DGs	size range of SCs
IEEE -119	case-17/ 17a	2	2	0-18.9MW	0-14.2MVAR
	case-18/ 18a	3	3	0-18.9MW	0-14.2MVAR
	case-19/ 19a	4	4	0-18.9MW	0-14.2MVAR
	case-20/ 20a	6	6	0-18.9MW	0-14.2MVAR

With the increase of the nodes, IEEE-119 bus distribution network is more complex, so that the configuration of multiple DGs and SCs is more difficult.

In order to verify the superiority of the new improved algorithm, four groups of comparative experiments are carried out in the IEEE-119 system. The detailed information of DGs/SCs on IEEE-119 nodes under various research conditions is provided in TABLE VII.

Fig. 14 shows the distribution of sensitivity factors of reactive power net loss at each node, among them, nodes with large sensitivity factors are distributed in a concentrated manner, and these points will also be selected preferentially. In complex large system computation, the search space and computational complexity of intelligent algorithm can be greatly reduced in this way.

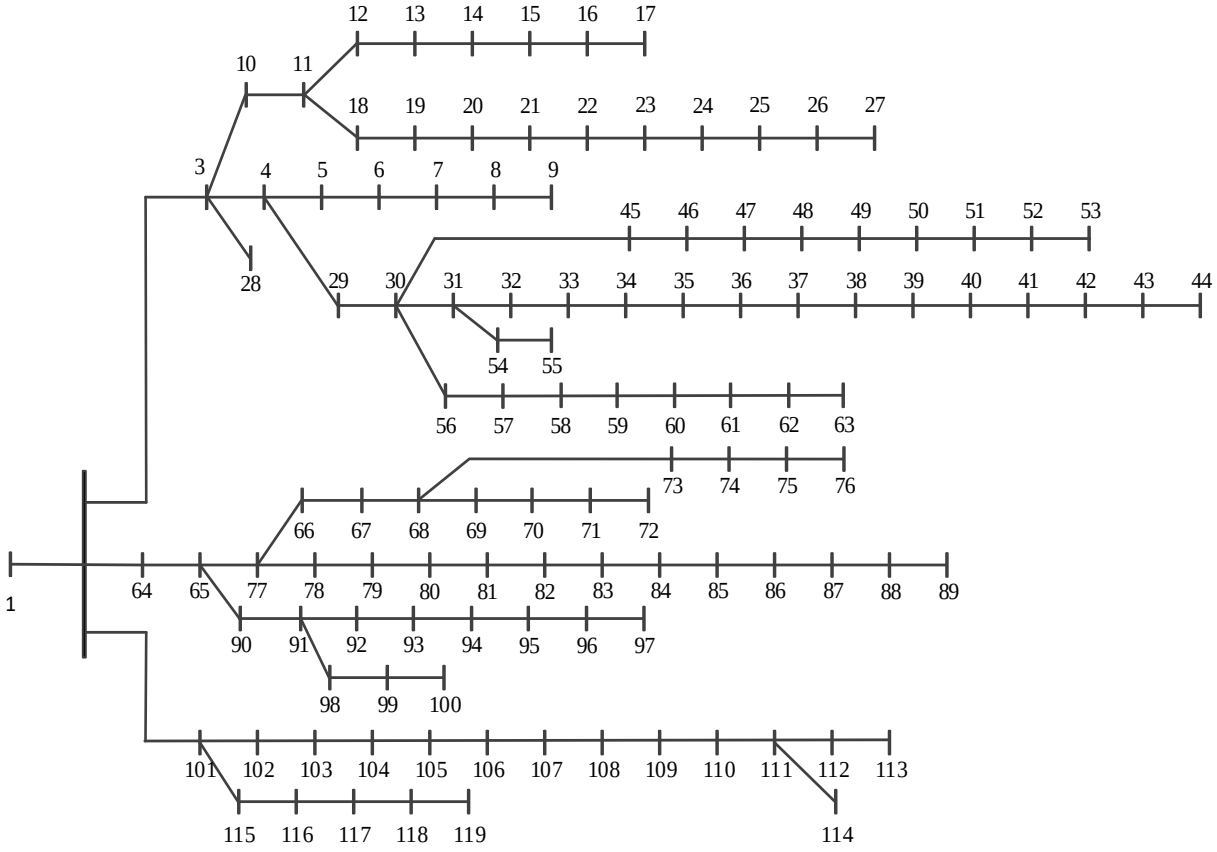

Fig. 13. IEEE-119 bus test system

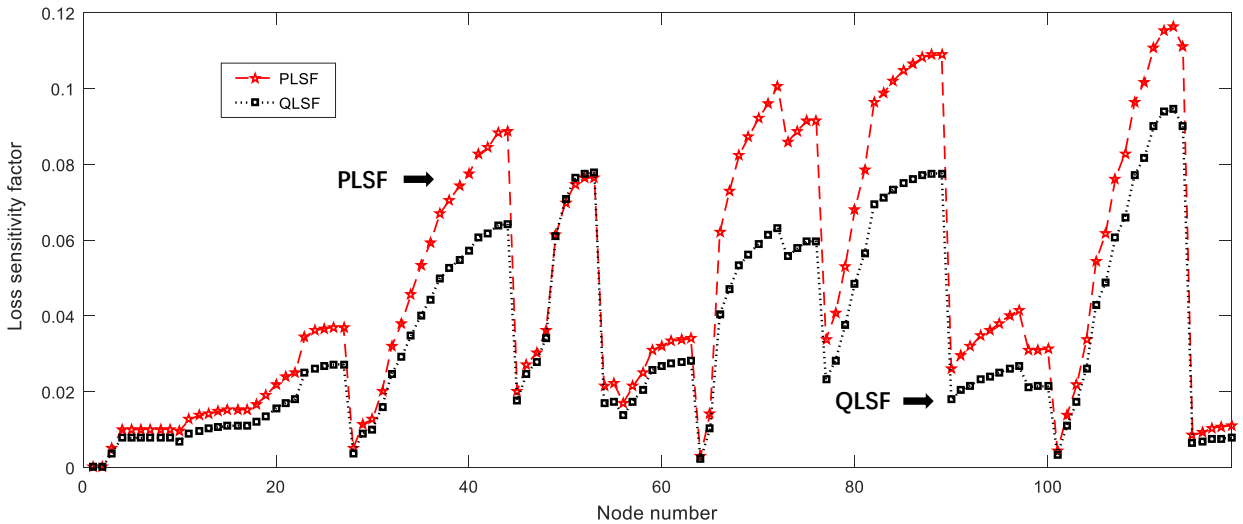

Fig. 14. Distribution of sensitivity factors in IEEE-119

TABLE VIII indicates the design schemes of 2 DGs+2 SCs (case-17/case-17a) and 3 DGs+3 SCs (case-18/case-18a) and so on. In case-17 and case-18, all nodes selected are from the top 30 percent of the sensitivity factors, such as node 111 ranked 4, node 85 ranked 9 and node 40 ranked 30. In case-20, all nodes are in the top 30 percent of sensitivity analysis, except node 96, which ranked 51. It proves that introducing sensitivity analysis into the algorithm can greatly simplify the search space. However, in the traditional PSO algorithm, when there are only two DGs and SCs with fewer parameters, the same results (case-17 and case-17a) can be obtained as the optimized algorithm. With the increase of optimization parameters, PSO will choose nodes with relatively small sensitivity as candidate points due to the absence of guiding factors, which are prone to fall into local optimization and fail to get better results.

Fig. 15 shows a comparison of the voltage levels of each node of the system after the optimized configuration. Comparing the two algorithms, it can be concluded that the PSO-OS algorithm can control the overregulation better under the premise of greatly improving the voltage level of the grid in the case of the same number of SCs and DGs. For example, by comparing the results of case-20 and case-20a, it can be found that the voltage result curve of the improved PSO-OS algorithm is closer to 1 *p.u.* and the maximum voltage of 1.0037 *p.u.* at node 40 is better than that of 1.0242 *p.u.* at node 44 of the traditional PSO algorithm.

TABLE IX details the comparison of the final experimental results under various conditions. In case-18 and case-18a, the PSO-OS algorithm reduces the active power network loss by 3.79% and the reactive power network loss by 3.54% compared with PSO algorithm. In case-20 and case-20a, the numbers are 10.84% and 6.33%. It is worth noting that in case-19 and case-19a, although the PSO algorithm has well control of minimum voltage and reactive power network loss, excessive voltage oversetting is a fatal disadvantage. With the increase of DGs and SCs, the optimization parameters increase, which makes the improved algorithm more and more advantageous over the traditional algorithm.

TABLE VIII
CONFIGURATION RESULTS FOR IEEE-119 SYSTEM

case no. (PSO-OS)	active power of DGs in KW (node)	reactive power of SCs in KVAR (node)	case no. (PSO)	active power of DGs in KW (node)	reactive power of SCs in KVAR (node)
case-17	2401(84), 3014(112)	1699(84), 2468(112)	case-17a	2401(84), 3014(112)	1699(84), 2468(112)
case-18	3343(40), 2309(85) 3126(111)	3785(40), 1631(85) 2554(111)	case-18a	3105(42), 1988(82) 3427(108)	3912(42), 1652(82) 2208(108)
case-19	3123(40), 1844(64) 3208(73), 2851(111)	2703(40), 1203(64) 2479(73), 2220(111)	case-19a	3425(42), 2013(50) 2920(87), 3008(109)	2641(42), 1632(50) 2537(87), 2508(109)
case-20	3105(40), 2128(52) 3215(73), 1860(84) 1312(96), 2839(111)	2698(40), 1199(52) 2485(73), 1181(84) 1651(96), 2247(111)	case-20a	2654(44), 2425(51) 2984(71), 2035(85) 1650(98), 2468(111)	2864(44), 1685(51) 2168(71), 1349(85) 1969(98), 2196(111)

TABLE IX
COMPARISON OF PSO-OS AND PSO ALGORITHMS FOR IEEE-119 SYSTEM

case no.	Max bus voltage in p.u.(node)	Min bus voltage in p.u.(node)	Real power loss in KW	Real power loss reduction	reactive power loss in KVAR	Reactive power loss reduction
base	1(1)	0.9293 (113)	978	--	718.8	--
case-17	1.007 (84)	0.9327 (44)	592.8	39.39%	472.2	34.31%
case-17a	1.007 (84)	0.9327 (44)	592.8	39.39%	472.2	34.31%
case-18	1.017 (40)	0.9475 (54)	446.8	54.31%	302.2	57.96%
case-18a	1.024 (42)	0.9473 (54)	483.9	50.52%	327.6	54.42%
case-19	1.004 (40)	0.9458 (89)	371	62.07%	253.9	64.68%
case-19a	1.0413 (87)	0.9521 (72)	413.4	57.73%	254.8	64.55%
case-20	1.0037 (40)	0.9736 (27)	184.7	81.11%	123.9	82.76%
case-20a	1.0242 (44)	0.9735 (27)	290.8	70.27%	169.4	76.43%

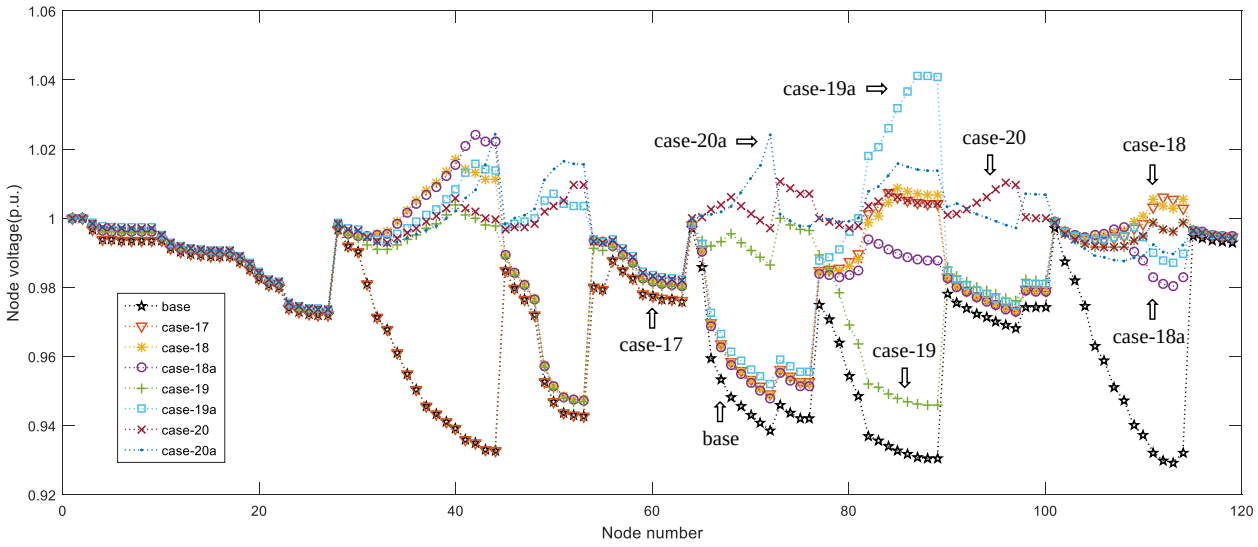

Fig. 15. Voltage distribution in IEEE-119

TABLE X
COMPARISON OF PSO-OS AND PSO ALGORITHMS FOR IEEE-119 SYSTEM

IEEE-119	case-17		case-18		case-19		case-20	
	PSO-OS	PSO	PSO-OS	PSO	PSO-OS	PSO	PSO-OS	PSO
worst result (KW)	593.9	595.5	453.1	510.3	384.6	454.7	187.9	358.8
best result (KW)	592.8	592.8	446.8	483.9	372.2	413.9	184.7	290.8
average (KW)	593.3	594.3	449.2	498.8	376.9	425.6	186.1	314.8
variance	0.1091	0.4127	4.5881	52.58	13.9664	79.248	33.5257	254.09

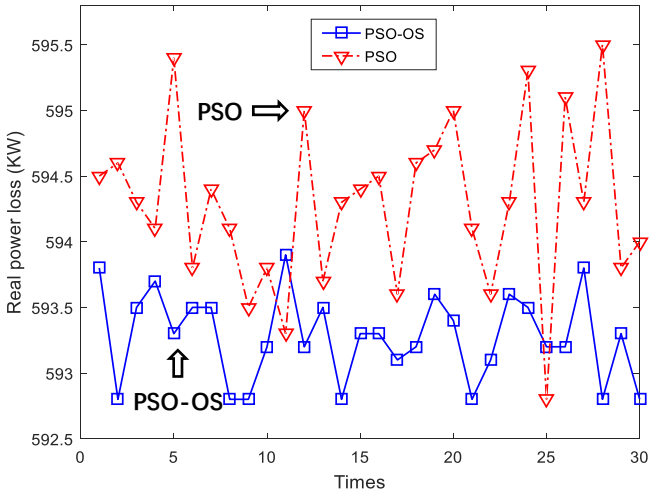

Fig. 16. The results' distribution for case-17 and case-17a of IEEE-119 test system

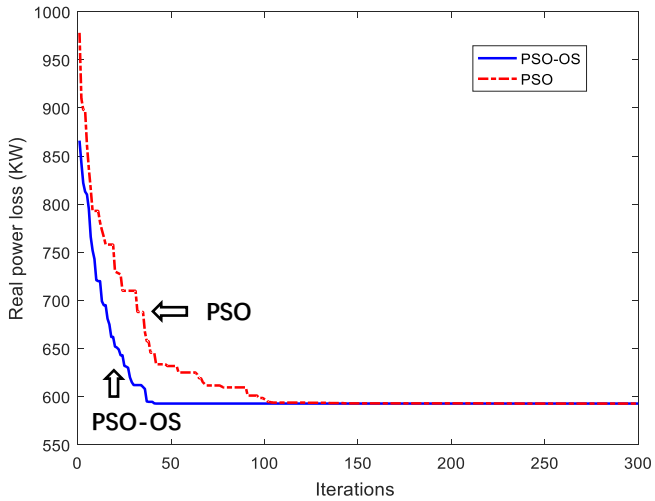

Fig. 17. The optimal convergence curves for case-17 and case-17a

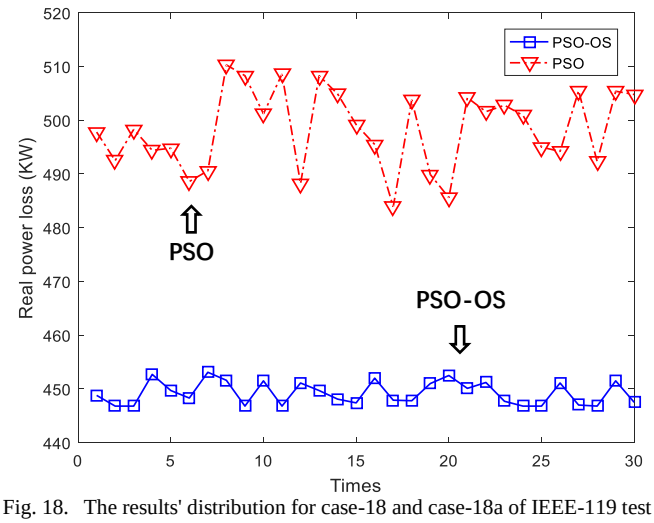

Fig. 18. The results' distribution for case-18 and case-18a of IEEE-119 test system

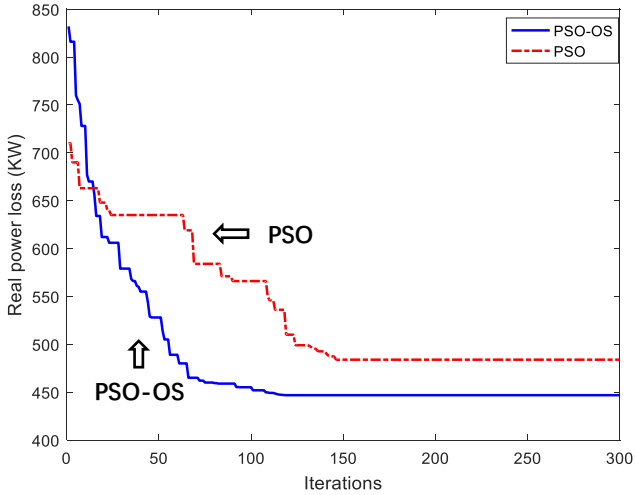

Fig. 19. The optimal convergence curves for case-18 and case-18a

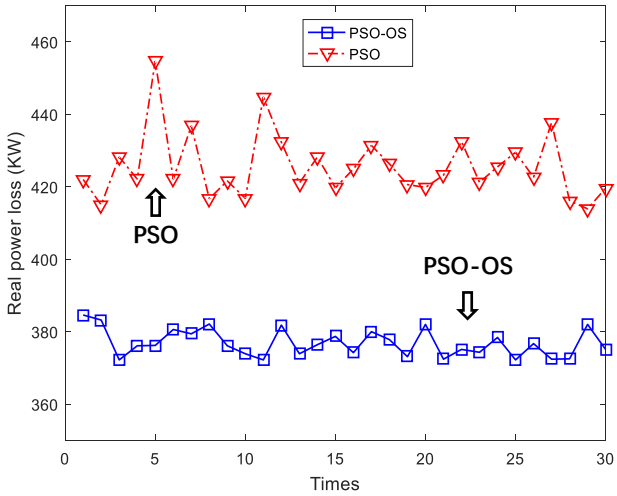

Fig. 20. The results' distribution for case-19 and case-19a of IEEE-119 test system

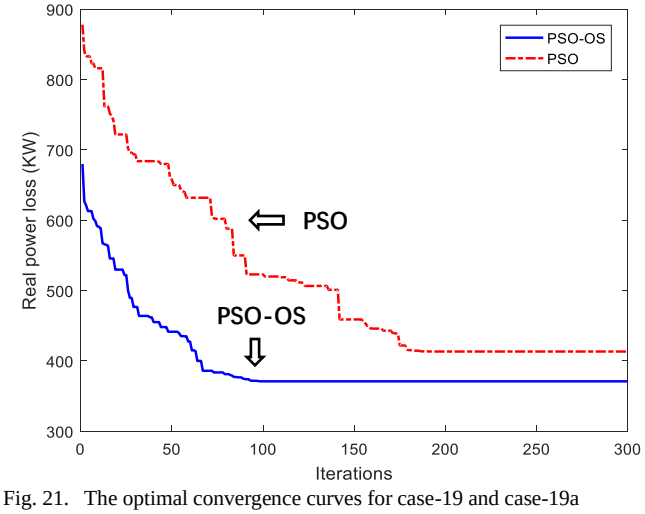

Fig. 21. The optimal convergence curves for case-19 and case-19a

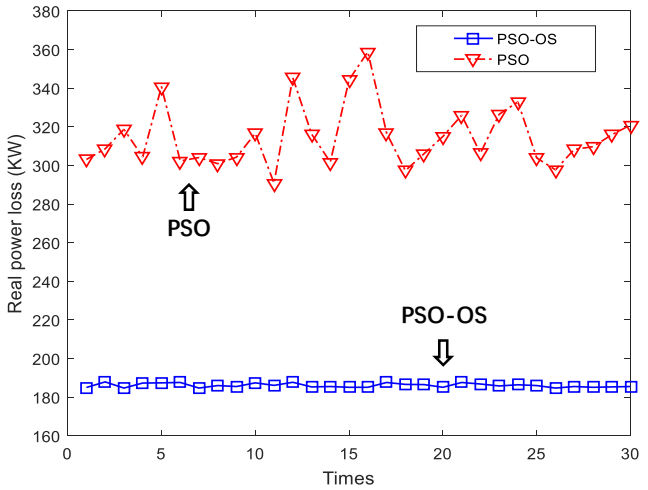

Fig. 22. The results' distribution for case-20 and case-20a of IEEE-119 test system

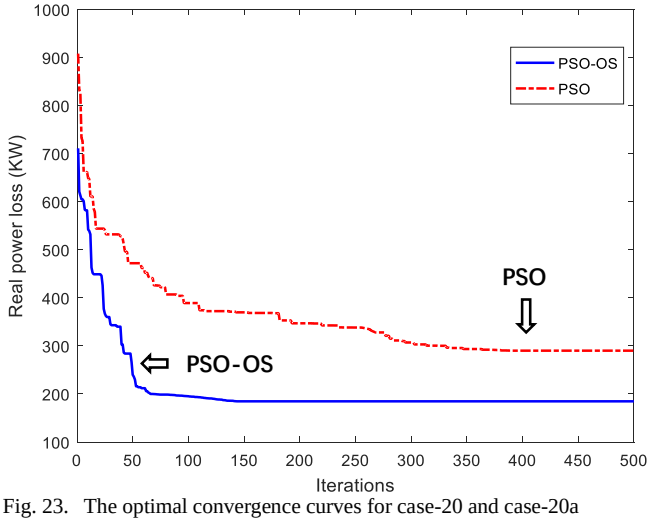

Fig. 23. The optimal convergence curves for case-20 and case-20a

The convergence speed and robustness of the algorithm are both important indexes to evaluate the algorithm. In order to verify the superiority of the improved algorithm, this paper carried out independent repeated experiments on PSO and PSO-OS for 30 times respectively, and selected the best results for comparative analysis of iterative curves. And the specific iteration results are recorded as shown in TABLE X

Fig. 16 shows the results of 30 independent replications for case-17 and case-17a of IEEE-119 test system. It can be seen that under the premise of fewer control variables, the active power network loss of the system obtained by the traditional PSO algorithm in only the 11th and 25th experiments are slightly better than that of the PSO-OS algorithm. In addition, the performance of the improved algorithm in terms of mean value, stability and the worst results is superior.

Fig. 17 illustrates the comparison of the two optimal iterative curves. Due to the introduction of the guidance factor, the PSO-OS algorithm converges in generation 43, while the traditional PSO algorithm gradually converges after generation 140.Furthermore, in the convergence process, the traditional PSO algorithm mainly relies on random numbers to determine the candidate nodes of DGs and SCs. In the large system with 119 nodes, most of the search work is inefficient, which leads to the difficulty in convergence of this algorithm and further causes the algorithm to take too long time.

With the increase in the number of DGs and SCs, the improved algorithm obtained from 30 repeated experiments has been superior to the traditional PSO algorithm in all aspects in Fig. 18 and Fig.20. On the other hand, the comparison of two optimal iterative curves in Fig. 19 and Fig. 21 also shows that PSO-OS algorithm is more suitable for this system.

As the control variables of the system increase, the computational complexity of the algorithm increases exponentially. The traditional PSO algorithm is easy to fall into the local optimal solution and cannot jump out easily. It should be noted that in the DG capacity result calculated by PSO algorithm in Fig. 22, the capacity will be infinitely close to 0 which is obviously the result of failure. In 30 independently repeated experiments, this happened 6 times, which once again proved the necessity of algorithm improvement. The experimental results show that the proposed PSO-OS algorithm can successfully solve the optimization problem in the larger radial distribution system.

In Fig. 23, it takes 381 iterations for PSO algorithm to converge to the active power loss of 290.07 kW, while the improved PSO-OS algorithm only took 124 generations of iterations to converge to the active power loss of 184.7 kW. It can be seen that the performance of both timeliness and accuracy algorithms has been greatly improved.

V. Conclusion

DGs and SCs are playing an increasingly important role in power system and with the selection of simultaneous optimal capacity and location of DGs and SCs, not only the power loss of radial distribution network is reduced, but also the voltage profile is enhanced. In this new proposed PSO-OS algorithm, an efficient approach that introduce active and reactive power loss sensitivity analysis to conduct variation of place parameters in standard PSO to increase algorithm search efficiency. Shrinking factor is proposed to balance the influence of learning factors and control the flying speed of particles. The advantages of PSO-OS can be summarized as follows: (1) The optimal combination of DGs/SCs positions and capacities can be directly calculated by the algorithm. The candidate position and capacity are optimized separately within the algorithm, which optimizes the search space and improves the search efficiency. (2) Sensitivity factor analysis is introduced to simplify the search space dimension and reduce the convergence time of the algorithm. (3) The shrinkage factor is introduced to ensure the accuracy and improve the efficiency of optimization. The superiority of the PSO-OS is demonstrated on IEEE-33 and IEEE-69 and IEEE-119 test system distribution networks and the simulation results are presented. By comparing the results of various algorithms in the previous literature, it can be known that PSO-OS can find solutions with lower active power loss and higher voltage level under various cases. Compared with the algorithm before the improvement, the PSO-OS algorithm has better convergence and stronger optimization ability. Thus, this can reduce the loss of electricity and improve energy utilization effectively. At the same time, the stability of RDN is enhanced.

References

[1]. P. Prakash and D.K. Khatod, "Optimal sizing and siting techniques for distributed generation in distribution systems: A review," *Renewable & Sustainable Energy Reviews*, vol. 57, pp. 111-130, 2016.

[2] P.S. Georgilakis and N.D. Hatziargyriou, "Optimal distributed generation placement in power distribution networks: models,

methods, and future research," *IEEE Transactions on Power Systems*, vol. 28, pp. 3420-3428, 2013.
[3] D.Q. Hung, N. Mithulananthan and R.C. Bansal, "Analytical expressions for DG allocation in primary distribution networks," *IEEE Transactions on Energy Conversion*, vol. 25, pp. 814-820, 2010.
[4] N. Khalesi, N. Rezaei and M.R. Haghifam, "DG allocation with application of dynamic programming for loss reduction and reliability improvement," *International Journal of Electrical Power & Energy Systems*, vol. 33, pp. 288-295, 2011.
[5] M. Ettehadi, H. Ghasemi and S. Vaez-Zadeh, "Voltage stability-based DG placement in distribution networks," *IEEE Transactions on Power Delivery*, vol. 28, pp. 171-178, 2013.
[6] M. Katsanevakis, R. Stewart and J. Lu "A novel voltage stability and quality index demonstrated on a low voltage distribution network with multifunctional energy storage systems," *Electric Power Systems Research*, vol. 171, pp. 264-282, 2019.
[7] V. Tamilselvan, T. jayabarathi, T. Raghunathan and X.S. Yang, " Optimal capacitor placement in radial distribution systems using flower pollination algorithm," *Alexandria Engineering Journal*, vol. 57, pp. 2775-2786, 2018.
[8] Y.M. Shuaib, M.S. Kalavathi and C.C.A. Rajan, "Optimal capacitor placement in radial distribution system using gravitational search algorithm," *International Journal of Electrical Power & Energy Systems*, vol. 64, pp. 384-397, 2015.
[9] S. Das, D. Das and A. Patra, "Operation of distribution network with optimal placement and sizing of dispatchable DGs and shunt capacitors," *Renewable and Sustainable Energy Reviews*, vol. 113, pp. 209-219, 2019.
[10] L.F. Ochoa, A. Padilhafeltrin and G.P. Harrison, "Evaluating distributed generation impacts with a multiobjective index," *IEEE Transactions on Power Systems*, vol. 21, pp. 1452-1458, 2006.
[11] Y.M. Atwa, E.F. El-Saadany, and M.M.A. Salama, "Optimal renewable resources mix for distribution system energy loss minimization," *IEEE Transactions on Power Systems*, vol. 25, pp. 360-370, 2010.
[12] G. Chen, J. Cao, Z. Zhang, and Z. Sun, "Application of Imperialist Competitive Algorithm with Its Enhanced Approaches for Multi-Objective Optimal Reactive Power Dispatch Problem," *Engineering Letters*, vol. 27, no. 3, pp. 579-592, 2019.
[13] K.Y. Chan, G.T.Y. Pong and K.W. Chan, "Investigation of Hybrid Particle Swarm Optimization Methods for Solving Transient-Stability Constrained Optimal Power Flow Problems," *Engineering Letters*, vol. 16, no. 1, pp. 61-67, 2008.
[14] G. Chen, S. Qiu, Z. Zhang, and Z. Sun, "Quasi-oppositional cuckoo search algorithm for multi-objective optimal power flow," *IAENG International Journal of Computer Science*, vol. 45, no. 2, pp. 255-266, 2018.
[15] F.S. Abu-Mouti and M.E. El-Hawary, "Optimal distributed generation allocation and sizing in distribution systems via artificial bee colony algorithm," *IEEE Transactions on Power* Delivery vol. 26, pp. 2090-2101, 2011.
[16] T.R. Ayodele, A.S.O. Ogunjuyigbe and O.O. Akinola, "Optimal location, sizing, and appropriate technology selection of distributed generators for minimizing power loss using genetic algorithm," *Journal of Renewable Energy*, vol. 2015, pp. 1-9, 2015.
[17] S. Kansal, V. Kumar and B. Tyagi, "Hybrid approach for optimal placement of multiple DGs of multiple types in distribution networks," *International Journal of Electrical Power & Energy Systems*, vol. 75, pp. 226-235, 2016.
[18] D.R. Prabha, T. Jayabarathi, R. Umamageswari, and S. Saranya. "Optimal location and sizing of distributed generation unit using intelligent water drop algorithm," *Sustainable Energy Technologies & Assessments*, vol. 11, pp. 106-113, 2015.
[19] E. Fergany and A. Attia, "Optimal allocation of multi-type distributed generators using backtracking search optimization algorithm," *International Journal of Electrical Power & Energy Systems*, vol. 64, pp. 1197-1205, 2015.
[20] S. Das, D. Das and A. Patra, "Operation of distribution network with optimal placement and sizing of dispatchable DGs and shunt capacitors," *Renewable and Sustainable Energy Reviews*, vol. 113, pp. 209-219, 2019.
[21] P.P. Biswas, R. Mallipeddi, and P.N. Suganthan, "A multiobjective approach for optimal placement and sizing of distributed generators and capacitors in distribution network," *Applied Soft Computing*, vol. 60, pp. 268-280, 2017.
[22] P. Lazzeroni and M. Repetto, "Optimal planning of battery systems for power losses reduction in distribution grids," *Electric Power Systems Research*, vol. 167, pp. 94-112, 2019.
[23] D.Q. Hung, N. Mithulananthan and R.C. Bansal, "Analytical expressions for DG allocation in primary distribution networks," *IEEE Transactions on Energy Conversion*, vol. 25, pp. 814-820, 2010.
[24] S.G. Naik, D.K. Khatod and M.P. Sharma, "Optimal allocation of combined DG and capacitor for real power loss minimization in distribution networks," *International Journal of Electrical Power & Energy Systems*, vol. 53, pp. 967-973, 2013.
[25] J. Kennedy and R. Eberhart, "Particle swarm optimization," *Proceedings of ICNN'95 - International Conference on Neural Networks*, Australia Council, Perth, 1995.
[26] M.E. Baran and F.F. Wu, "Network reconfiguration in distribution systems for loss reduction and load balancing," *IEEE Transactions on Power Delivery*, vol. 4, pp. 1401-1407, 1989.
[27] R. Baghipour and S.M. Hosseini, "Placement of DG and capacitor for loss reduction, reliability and voltage improvement in distribution system using BPSO," *International Journal of Intelligent Systems & Applications*, vol. 12, pp. 57-64, 2012.
[28] N. Kanwar, N. Gupta, and K.R. Niazi, "Improved meta-heuristic techniques for simultaneous capacitor and DG allocation in radial distribution networks," *International Journal of Electrical Power & Energy Systems*, vol. 73, pp. 653-664, 2015.
[29] A. Khodabakhshian and M.H. Andishgar, "Simultaneous placement and sizing of DGs and shunt capacitors in distribution systems by using IMDE algorithm," *International Journal of Electrical Power & Energy Systems*, vol. 82, pp. 599-607, 2016.
[30] K. Muthukumar and S. Jayalalitha, "Optimal placement and sizing of distributed generators and shunt capacitors for power loss minimization in radial distribution networks using hybrid heuristic search optimization technique," *International Journal of Electrical Power & Energy Systems*, vol. 78, pp. 299-319, 2016.
[31] I.A. Mohamed and M. Kowsalya, "Optimal distributed generation and capacitor placement in power distribution networks for power loss minimization," *2014 International Conference on Advances in Electrical Engineering (ICAEE)*, Vellore, India, 2014.
[32] M.M. Aman, G.B. Jasmon, and A.H.A. Bakar, "Optimum network reconfiguration based on maximization of system loadability using continuation power flow theorem," *International Journal of Electrical Power & Energy Systems*, vol. 54, pp. 123-133, 2014.